Shape recovery from images acquired by a wedge-ring poor-pixels detector

Wen Pengcheng[1], Zhang Yadi[1], Wang Xiangjun[2], Wei Hong[3]

(1. AVIC Computing Technique Research Institute, Xi'an 710119, China;
2. College of Precision Instrument and Opto-Electronics Engineering, Tianjin University, Tianjin 300072, China;
3. School of Systems Engineering, University of Reading, Reading RG6 6AY, UK)

Abstract: A novel wedge-ring poor-pixels photoelectric detector is valuable for a micro vision system. However an image acquired by the detector has extremely low resolution and it does not reflect the same or similar shape information of an object in the real world. To enable such a detector and its images available in further object identification, a unique shape recovery framework was presented in this paper. By rotating the wedge-ring detector around its center in a sub-wedge range, original low-resolution images were generated. Then linear interpolation along with a least squares method was applied to preliminarily recover the object shape. After noise removal via a two-stage level set evolution with an edge indicator function, the final high-quality object shape was achieved. Experiments demonstrate the effective performance of the proposed algorithms, in which the shape recovery rate is up to 95%.

Key words: shape recovery; poor-pixels detector; wedge-ring image; linear interpolation; level set evolution

CLC number: TN911.7 Document code: A Article ID: 1007-2276(2013)05-1366-06

楔环贫点阵探测器图像的形状恢复方法

文鹏程[1],张亚棣[1],王向军[2],卫 红[3]

(1. 中航工业西安航空计算技术研究所,陕西 西安 710119;
2. 天津大学 精密仪器与光电子工程学院,天津 300072;
3. 英国雷丁大学 系统工程学院,英国雷丁 RG6 6AY)

摘 要:新型楔环贫点阵光电探测器有利于微小型视觉系统的实现,然而它采集的图像分辨率极低,不能反映与目标外在形状相同或相近的特征。为了使该探测器及其图像能够应用于目标识别,提出一种独特的形状恢复方法。以楔环中心为原点旋转探测器,获取一系列原始低分辨率图像,通过最小二乘线性插值对目标形状进行初步恢复,利用嵌入边缘指示函数的两级水平集演化算法去除图像噪声,可得到最终的高质量的目标形状。实验表明,文中提出的形状恢复方法行之有效,形状恢复率达 95%。

关键词:形状恢复; 贫点阵探测器; 楔环图像; 线性插值; 水平集演化

收稿日期:2012-09-12; **修订日期**:2012-10-17

基金项目:国家自然科学基金(60872097)

作者简介:文鹏程(1981-),男,博士,主要从事计算机视觉、图形图像处理、模式识别等方面的研究。

Email:victorlionwen@hotmail.com

0 Introduction

A novel wedge-ring detector, with extremely small quantity of pixels on its imaging surface, is designed for an embedded computer vision system. It is valuable in many applications such as micro unmanned aerial vehicles for military or civil undercover surveillance and micro biomimetic robots for medical observation inside the delicate pipe tissues, e.g. blood vessels. Stemming from the human vision, the detector is of a round shape with photosensitive cells(pixels) distributed symmetrically to its center as well as to its axis. Usually the number of the cells is less than one hundred. Advantages of such kind of detector are as follows.

(1) A few photosensitive cells ensure the detector miniature in size, light in weight, and less power-consumption, which are helpful in a highly-integrated battery-using system. Meanwhile, the image acquisition speed is dramatically accelerated due to only a few photoelectric signals being processed[1].

(2) The detector is designed in a wedge-ring shape in accordance with the human vision system in which photoreceptors placed on the retina are grouped as inner to outer rings[2]. This type of pixel distribution benefits the post image processing by using a logarithmic-polar transformation algorithm from its polar sampling[3-4].

As an example, an image captured by the 25-pixel wedge-ring detector, shown in Fig.1, has the following features. (1) It is an extremely low-resolution image, like a mosaic image. (2) Pixel size of the wedge-ring image varies, and grey information represented by these pixels is not with smooth continuity. Hence, the contexture information among pixels is hard to establish. An extremely low-resolution wedge-ring image does not reflect the same or similar shape information of an object in the real world. It is therefore difficult to identify an object based on such a single image.

Fig.1 Extremely low-resolution wedge-ring image with 25 pixels

To ensure the application of the wedge-ring detector in real problems, a unique framework is presented in ths paper specifically for shape recovery from extremely low-resolution wedge-ring images. It consists of three parts. In the first part, a simple and effective model is formulated, in which a series of original low-resolution images are acquired purely based on rotations around the center of the wedge-ring detector in a sub-wedge range. Usually the detector's center matches approximately together with the object's shape center after pre detecting and tracking. This operation, which is totally achievable in practice[5-6], takes account of the detector's particular pixel distribution. It is different from the traditional approaches working to regularly gridded detectors[7-9], since there is not a base for grid alignment if the wedge-ring detector which is of a round shape is also horizontally or vertically shifted up to a sub-pixel level to obtain multiple low-resolution images. In the second part of the framework, linear interpolation using a least squares method is applied to enhance image resolution and preliminarily recover the object shape. In the third part, a two-stage level set evolution with an edge indicator function is developed for further noise removal. The modification, which achieves a smooth model with non-trivial steady states, not only guarantees the whole denoising effect but also preserves the local edge information. Finally a high-quality object shape is obtained.

The rest of the paper is organized as follows. Section 1 introduces details of the proposed framework. Experimental results on synthetic images

are presented and discussed in Section 2. Section 3 concludes the work with identified achievements.

1 Methodology

1.1 Mathematical model

As a simple example, by rotating a wedge-ring detector around its center in a small angle θ, ranging from 0 to $\pi/4$, two extremely low-resolution wedge-ring images are acquired. As shown in Fig.2, they are represented by solid and dashed lines, respectively.

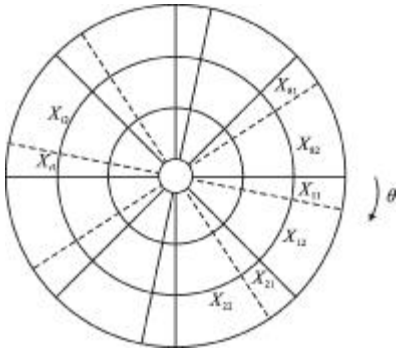

Fig.2 Modelling the resolution enhancement problem based on two extremely low-resolution wedge-ring images

Each image has three rings and eight pixels on each ring plus a central pixel. Based on these, the following relationship can be established:

$$\begin{bmatrix} Y_1 \\ Y_2 \end{bmatrix} = \begin{bmatrix} A_1 \\ A_2 \end{bmatrix} \begin{bmatrix} \mathbf{X}_{11} \\ \mathbf{X}_{12} \\ \vdots \\ \mathbf{X}_{81} \\ \mathbf{X}_{82} \end{bmatrix} \tag{1}$$

where Y_1, Y_2 are 8×3 matrices denoting low-resolution images. It is worth to note that only 24-pixel values for each measured image are used, and the central pixel value is not involved in calculation, for it keeps unchanged in the rotation. Even though there is a coincidence error caused by translations, the error is minor considering the much higher image acquisition speed and the relatively lower object movement speed. Then the calculation influence can be ignored. X_{ij} ($i=1,2,\cdots 8$, $j=1,2$) are 1×3 vectors denoting pixels needed to be recovered, and A_1, A_2 are coefficient matrices defined as:

$$A_1=R_1C_{12} \quad A_2=R_2C_{12} \tag{2}$$

$$C_{12}=\begin{bmatrix} \mathbf{p}_1 & \mathbf{p}_2 & 0 & 0 & 0 & \cdots & 0 \\ 0 & 0 & \mathbf{p}_1 & \mathbf{p}_2 & 0 & \cdots & 0 \\ \vdots & & & \ddots & & & \vdots \\ 0 & 0 & 0 & \cdots & 0 & \mathbf{p}_1 & \mathbf{p}_2 \end{bmatrix} \tag{3}$$

in which $\mathbf{R}_1$, $\mathbf{R}_2$ are rotation kernels and $\mathbf{p}_1$, $\mathbf{p}_2$ are weighting factors.

To extend the above example to $\mathbf{N}$ extremely low-resolution wedge-ring images, it is obtained as

$$\begin{bmatrix} Y_1 \\ \vdots \\ Y_N \end{bmatrix} = \begin{bmatrix} R_1C_{1N} & & \\ & \ddots & \\ & & R_NC_{1N} \end{bmatrix} \begin{bmatrix} X_{11} \\ \vdots \\ X_{1N} \\ \vdots \\ X_{ij} \\ \vdots \\ X_{81} \\ \vdots \\ X_{8N} \end{bmatrix} = \begin{bmatrix} A_1 & & \\ & \ddots & \\ & & A_N \end{bmatrix} \begin{bmatrix} X_{11} \\ \vdots \\ X_{1N} \\ \vdots \\ X_{ij} \\ \vdots \\ X_{81} \\ \vdots \\ X_{8N} \end{bmatrix} \rightarrow Y=AX \tag{4}$$

where

$Y=[Y_1^T,\cdots,Y_N^T]^T$ of size $8\mathbf{N}\times3$,

$X=[X_{11}^T,\cdots,X_{1N}^T,\cdots,X_{ij}^T,\cdots,X_{81}^T,\cdots,X_{8N}^T]^T$, $A=[A_1^T,\cdots,A_N^T]^T$ of size $8\mathbf{N}\times8\mathbf{N}$.

If $\mathbf{N}$, which is also regarded as the rotation times within a $\pi/4$ angle, is sufficiently large, by solving the linear Equation(4), a high-resolution image can be recovered theoretically.

1.2 Linear interpolation

To calculate the inverse matrix A^{-1} is a direct way to solve Equation(4). Unfortunately, some rows in the matrix A are linearly dependent in light of the particular rotation model. A does not have full rank and is then singular. Therefore, A^{-1} does not exist and Equation(4) does not have a unique solution.

To address this ill-posed problem, a least squares method is adopted to compute the best fit solution. Equation (4) is rewritten as the following optimal estimation:

$$\hat{X}=\arg\min_{\mathbf{x}} \| AX-T \|_2 \tag{5}$$

where $\hat{\mathbf{X}}$ denotes an optimal estimate and $\|\cdot\|_2$ denotes the L2 norm. Equation(5) seeks a matrix $\hat{X}$ that minimizes the Euclidean distance between AX and Y. To achieve this goal, $A^+=\lim_{\sigma\to 0}(A^TA+\sigma I)^{-1}A^T$ is used to replace A^{-1} to solve Equation(4), where I is an identity matrix and σ is a very small positive value close to 0. The limit process ensures that A^+ always exists.

Although the above method is easy to operate and workable as well, the condition number $\mathbf{K}(A)$ of matrix A in practice is large, which makes the least squares solution to Equation(4) become ill-conditioned. Under this circumstance, small errors in entries of A will be enlarged in the solution $\hat{X}$. Consequently, a mass of extra noises would appear in the restored high-resolution image. To improve the final output, a modified level set evolution is developed for further noise removal.

1.3 Noise removal

Among all filtering techniques, level set methods have become popular as they are less sensitive to natural noise and more contrast preserving. The evolution equation of the level set function φ can be written as[10]:

$$\frac{\partial \varphi}{\partial t}+\mathbf{F}|\nabla \varphi|=0 \tag{6}$$

where $\mathbf{F}$ is a speed function determining the diffusion of the moving interface. For the problem of noise removal, φ is replaced by the image data $\mathbf{I}_m$, and $\mathbf{F}$ is a kind of curvature flows selected according to the principles introduced in Ref.[11]. This approach has shown good performance on the denoising effect in very noisy images. However, it only penalizes high curvature value regardless of the curve regularity, which may cause edge blurring and limit its capability to shape recovery.

To preserve more edge information, an edge indicator function $\mathbf{g}$ is added to work along with the evolution process. $\mathbf{g}$ can be defined as[12]:

$$\mathbf{g}=\frac{1}{1+|\nabla \mathbf{G}_\sigma\cdot\mathbf{I}_m|^2} \tag{7}$$

where $\mathbf{G}_\sigma$ is the Gaussian kernel with standard deviation $\sigma>0$. Let

$$\mathbf{F}'=\mathbf{g}\cdot\mathrm{div}\left(\frac{\nabla \mathbf{I}_m}{|\nabla \mathbf{I}_m|}\right) \tag{8}$$

replace the speed function $\mathbf{F}$ in Equation(6), where div(·) is a divergence operator. Although the details of the object edge are preserved well, this modification just drives the moving interface to diffuse in a local area, which may not be applicable to the full-image continuous noise.

Based on the characteristics of the interim image restored from Section1.2, a strategy of two-stage level set evolution is developed. At the first stage, the classic speed function $\mathbf{F}$ of mean / min / max curvature flows[11] is applied to control the evolution to remove noise in the whole image. This iterative smoothing should be stopped as soon as the scattered noise is disappeared. Usually it needs about fifty iterations in practice. At the second stage, the modified speed function $\mathbf{F}'$ takes over the responsibility of preserving the local edge information. The evolution can be stopped automatically, when the maximum difference between two consecutive images is less than a given threshold[13].

The strategy of two-stage level set evolution achieves a good compromise between noise removal in the whole image and edge preservation in the local area.

2 Experimental results

In this section, testing experiments on synthetic images are presented to demonstrate the effectiveness of the proposed shape recovery framework. All simulations are implemented in MATLAB.

Three round-shaped images with 7 213 pixels each are used in the testing, and objects contained in these images are "man", "airplane" and "car", as shown in Fig.3(a). For each of the images, $\mathbf{N}$ extremely low-resolution wedge-ring images are generated with rotation angles $\theta=\mathbf{n}\frac{\pi/4}{\mathbf{N}}$, ($\mathbf{n}=0,1,2,\cdots,\mathbf{N}-1$) and the down-sampling ratio $\alpha=\frac{7\,213}{25}$. Fig.3(b) shows the synthetic down-sampled images at $\theta=0$.

(a) Original images

(b) Examples of down-sampled low-resolution wedge-ring images at θ=0

(c) Preliminary shape recovery by linearly interpolating 200 down-sampled images

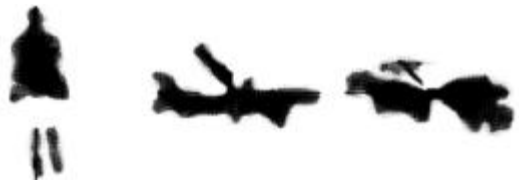

(d) Final outputs after noise removal via the two-stage level set evolution

Fig. 3 Results showing the proposed framework work to shape recovery

Based on a pre-observation, 200 extremely low-resolution wedge-ring images are used to preliminarily recover the object shape by linear interpolation. This is because there is a maximum to **N** in the initial recovery process, i.e. when **N** reaches its maximum, in this case about **N**=200, the recovered image quality will not be significantly improved by further increasing **N**. Main reasons are discovered as follows. (1) The down-sampling ratio is too high to make the measured data keep a great deal of information during the decimation process. (2) When **N** is large, the rotation angle becomes very small, which causes consecutive down-sampled images containing same information. As a result, contribution of these images to recovering the interim image is demolished. To be emphasized here, **N**=200 is also an optimum value for satisfying the processing speed requirement. Since the image acquisition speed is up to 2 000 frames/s using the designed wedge-ring detector [1], to acquire 200 images only needs 0.1 s. Adding the post processing time, it is acceptable to the whole shape recovery and object identification process. Fig.3(c) shows the results of preliminary shape recovery. After noise removal by the two-stage level set evolution, the final outputs are illustrated in Fig.3(d). It can be seen that the object shapes are recovered to a great extent compared with Fig.3(b) and Fig.3(c).

To quantitatively evaluate the accuracy of the shape recovery under the proposed framework, the parameter of similarity **S** in binary space is defined as:

$$\mathbf{S}=\left(1-\frac{\mathbf{P}_d}{\mathbf{P}_t}\right)\times 100\% \tag{9}$$

where $\mathbf{P}_d$ is the number of different pixels between the recovered object and the original object in binary space, and $\mathbf{P}_t$ is the number of total pixels, i.e. $\mathbf{P}_t$=7 213 in this experiment. Figure4 shows the comparative results, where light colour parts represent the different pixels. The quantitative results of the similarity are given in Tab.1. The over 91% of a minimum shape recovery rate is sufficient to further object identification in a log-polar space.

Fig.4 Comparison between the recovered object shapes and the original object shapes

Tab.1 Similarity between the recovered object shapes and the original object shapes

Object	Man	Airplane	Car
Similarity	91.10%	95.05%	92.22%

3 Conclusions

In this paper, a unique shape recovery framework is presented for extremely low-resolution wedge-ring images. Based on the mathematical formation of the wedge-ring pixel distribution, the linear interpolation working along with rotations around the center of the wedge-ring detector is applied for preliminary shape recovery. After further noise removal via the two-stage level set evolution, the final object shape can be recovered up to 95% of the original one. The experimental results have shown that the proposed framework is effectively performed in shape recovery specifically for extremely low-resolution wedge-ring images. It is a sensible step towards image understanding and object identification for micro wedge-ring detectors.

References:

[1] Wen P, Wang X. Multiprocessor poor pixels image acquisition system with low power consumption[J]. Chinese J Scientific Instrument,2006, 27(6): 1358-1359. (in Chinese)

[2] Snowden R, Thompson P, Troscianko T. Basic Vision-An Introduction to Visual Perception [M]. Oxford University Press Inc Oxford, 2006.

[3] Weiman C, Chaikin G. Logarithmic spiral grids for image processing and display [J]. Comput Graph Image Process, 1979, 11: 197-226.

[4] Sandini G, Tagliasco V. An anthropomorphic retina-like structure for scene analysis [J]. Comput Vis Graph Image Process, 1980, 14: 365-372.

[5] Watson B, Friend J, Yeo L. Piezoelectric ultrasonic resonant motor with stator diameter less than 250 μm: the proteus motor[J]. J Micromech Microeng, 2009, 19: 1-5.

[6] Guo Li, Ang Haisong, Zheng Xiangming. Video stabilization for micro air vehicle platform [J]. Infrared and Laser Engineering, 2012, 41(3): 696-703. (in Chinese)

[7] Elad M, Hel-Or Y. A fast super-resolution reconstruction algorithm for pure translational motion and comnmon space-invariant blur [J]. IEEE Trans Image Process, 2001, 10(8): 1187-1193.

[8] Farsiu S, Robinson M D, Elad M, et al. Fast and robust multiframe super resolution [J]. IEEE Trans Image Process, 2004, 13(10): 1327-1344.

[9] Zhang D, Li H, Du M. Fast MAP-based multiframe super-resolution image reconstruction[J]. Image Vis Comput, 2005, 23(7): 671-679.

[10] Osher S, Sethian J A. Fronts propagating with curvature-dependent speed: algorithms based on hamilton-Jacobi formulations[J]. J Comp Phys, 1988, 79: 12-49.

[11] Malladi R, Sethian J A. A unified approach to noise removal, image enhancement, and shape recovery [J]. IEEE Trans Image Process, 1996, 5(11): 1554-1568.

[12] Li C, Xu C, Gui C, Fox M D. Level set evolution without re-initialization: a new variational formulation[C]//IEEE Conf Computer Vision and Pattern Recognition, 2005: 1063-1069.

[13] Gil D, Radeva P. A regularized curvature flow designed for a selective shape restoration[J]. IEEE Trans Image Process, 2004, 13(11): 1444-1458.